The Journal of Experimental Biology 204, 431–442 (2001)
Printed in Great Britain © The Company of Biologists Limited 2001
JEB3056

WAKE DYNAMICS AND FLUID FORCES OF TURNING MANEUVERS IN SUNFISH

ELIOT G. DRUCKER[1,*] AND GEORGE V. LAUDER[2]

[1]*Department of Ecology and Evolutionary Biology, University of California, Irvine, CA 92697, USA* and
[2]*Museum of Comparative Zoology, Harvard University, 26 Oxford Street, Cambridge, MA 02138, USA*

*e-mail: edrucker@uci.edu

Accepted 3 November 2000; published on WWW 15 January 2001

Summary

While experimental analyses of steady rectilinear locomotion in fishes are common, unsteady movement involving time-dependent variation in heading, speed and acceleration probably accounts for the greatest portion of the locomotor time budget. Turning maneuvers, in particular, are key elements of the unsteady locomotor repertoire of fishes and, by many species, are accomplished by generating asymmetrical forces with the pectoral fins. The development of such left–right asymmetries in force production is a critical and as yet unstudied aspect of aquatic locomotor dynamics. In this paper, we measure the fluid forces exerted by the left and right pectoral fins of bluegill sunfish (*Lepomis macrochirus*) during turning using digital particle image velocimetry (DPIV). DPIV allowed quantification of water velocity fields, and hence momentum, in the wake of the pectoral fins as sunfish executed turns; forces exerted during turning were compared with those generated by the immediately preceding fin beats during steady swimming. Sunfish generate the forces required for turning by modulating two variables: wake momentum and pectoral fin stroke timing. Fins on opposite sides of the fish play functionally distinct roles during turning maneuvers. The fin nearer the stimulus inducing the turn (i.e. the strong side fin) generates a laterally oriented vortex ring with a strong central jet whose associated lateral force is four times greater than that produced during steady swimming. Little posterior (thrust) force is generated by the strong-side fin, and this fin therefore acts to rotate the body away from the source of the stimulus. The contralateral (weak-side) fin generates a posteriorly oriented vortex ring with a thrust force nine times that produced by the fin during steady swimming. Minimal lateral force is exerted by the weak-side fin, and this fin therefore acts primarily to translate the body linearly away from the stimulus. Turning with the paired fins is not simply steady swimming performed unilaterally. Instead, turning involves asymmetrical fin movements and fluid forces that are distinct in both direction and magnitude from those used to swim forward at constant speed. These data reflect the plasticity of the teleost pectoral fin in performing a wide range of steady and unsteady locomotor tasks.

Key words: manoeuvrability, turning, swimming, pectoral fin locomotion, flow visualization, digital particle image velocimetry, bluegill sunfish, *Lepomis macrochirus*.

Introduction

Experimental studies of animal movement have traditionally focused upon steady locomotor behaviors (i.e. involving rectilinear and constant-speed progression) either performed voluntarily or elicited by devices such as flow tanks, wind tunnels and treadmills. The benefit of this approach is the maintenance of control over the animal's direction and speed of translation. In spite of the focus on steady locomotion, however, such behavior probably constitutes only a relatively small fraction of any animal's locomotor time budget in nature (Harris, 1936; Aldridge, 1987; Fuiman and Webb, 1988; Webb, 1991; Eilam, 1994; Warrick, 1998; Dickinson et al., 2000). Instead, unsteady locomotion involving time-dependent variation in an organism's heading, speed and acceleration is probably the behavioral norm and, hence, of considerable ecological importance.

'Maneuverability' is a term used widely in the literature serving as a general descriptor for a variety of unsteady locomotor behaviors involving controlled, dynamic instability of the body. Among swimming animals, maneuvering performance has been evaluated in fishes both in terms of the ability to flex the body during turning (Gray, 1933; Weihs, 1972; Webb, 1983; Domenici and Blake, 1991; Blake et al., 1995) and to accelerate it during the fast-start (Harper and Blake, 1990; Domenici and Blake, 1991; Domenici and Blake, 1997; Kasapi et al., 1993; Webb, 1994) and in terms of the capacity to change the orientation and position of the body with the fins. The role of the paired pectoral fins of fishes has been the focus of several studies documenting maneuvers such as turning (Fricke and Hissmann, 1992; Gerstner, 1999), braking (Breder, 1926; Harris, 1937; Harris, 1938; Geerlink, 1987), negotiating obstacles (Webb et al., 1996; Schrank and Webb, 1998) and controlling vertical position in the water column (Blake, 1979; Arnold et al.,

1991; Wilga and Lauder, 1999; Wilga and Lauder, 2000). Recent work has also focused on unsteady pectoral fin movement as the basis of robotic fish design (Kato and Furushima, 1996; Kato, 1998; Kato, 1999). In most such studies, however, biomechanical arguments about how maneuvering is accomplished involve the inference of locomotor force from propulsor kinematics and hydrodynamic theory. There are essentially no empirical data on the potential differential contribution of the left- and right-side pectoral fins to unsteady locomotor behavior and, specifically, on the mechanical forces generated by fishes with their paired fins during maneuvering.

This study employs a quantitative flow-visualization technique, digital particle image velocimetry (DPIV), to provide empirical data on the mechanical forces generated by the pectoral fins during maneuvering in water. DPIV has been used to examine patterns of water flow in the wake of fishes swimming steadily (Müller et al., 1997; Drucker and Lauder, 1999; Drucker and Lauder, 2000; Lauder, 2000) and has also been applied to the dynamics of unsteady propulsion in teleost fishes (Wolfgang et al., 1999; Müller et al., 2000) and vertical maneuvering in sturgeon and sharks (Wilga and Lauder, 1999; Wilga and Lauder, 2000). However, the focus of DPIV studies of unsteady swimming has been on species for which axial undulation is the primary means of locomotion. As many as one-fifth of all living fishes rely instead primarily on their mobile and flexible pectoral fins for propulsion (Westneat, 1996). The generation of left–right force asymmetries by the paired fins is a critical and as yet unstudied aspect of locomotor dynamics. This study examines the forces involved in turning with the pectoral fins in the horizontal plane by a representative teleost labriform swimmer, the bluegill sunfish *Lepomis macrochirus*. By characterizing unsteady two-dimensional water velocity fields in the wake and by calculating from these data the forces exerted by each fin, we aim (i) to clarify the hydrodynamic mechanism of turning with the pectoral fins and to evaluate previous functional hypotheses based upon qualitative behavioral observations; and (ii) to quantify the extent to which turning and steady swimming differ biomechanically in order to assess the functional versatility of the teleost pectoral fin.

Materials and methods

Fish

Bluegill sunfish (*Lepomis macrochirus* Rafinesque) were selected for this study of turning to allow comparisons with previous work with this species on wake flow patterns during steady swimming (Drucker and Lauder, 1999; Drucker and Lauder, 2000). Experimental animals were maintained at 20 °C in 40 l freshwater aquaria and fed earthworms twice weekly. Four fish of similar size (total body length, L, 22.0±0.6 cm, mean ± S.D.) were used for wake visualization experiments.

Experimental protocol

Sunfish swam individually in the working area (28 cm×28 cm×80 cm) of a freshwater flow tank at a speed of $0.5\,L\,s^{-1}$ (approximately $11\,cm\,s^{-1}$), at which propulsion was achieved by oscillation of the pectoral fins alone. After swimming steadily for at least three consecutive strides, fish were induced to execute turns using the pectoral fins by means of a visual and auditory stimulus. Turns were elicited by directing a wooden dowel into the water and against the floor of the working area. The dowel was guided by hand along the inside wall of the flume (5–10 cm away from the tip of the abducted pectoral fin), so as to avoid interfering either with fin movements or with the resulting wake flow, and was introduced at a longitudinal position corresponding approximately to the location of the fish's head. To characterize the patterns of movement of the pectoral fins during turning, sunfish were videotaped from a ventral perspective at 250 frames s^{-1} using a NAC HSV-500 high-speed video system. These images were used for qualitative assessment of differential left–right fin movement during maneuvering.

Visualization of the pectoral fin wake was achieved in separate experiments by means of the DPIV system described in our previous work (Drucker and Lauder, 1999; Drucker and Lauder, 2000; Wilga and Lauder, 1999; Wilga and Lauder, 2000; Lauder, 2000). Reflective microspheres were seeded into the flow at a density of $14\,mg\,l^{-1}$ and illuminated by a 5 W continuous-wave argon-ion laser (Coherent, Inc., Santa Clara, CA, USA) focused into a thin sheet of light 17 cm wide. A dual-camera high-speed video system (NAC HSV-500c[3]) was used to record images of the fish and planar transections of its pectoral fin wake at 250 frames s^{-1} (1/500 s shutter speed). Previous work with *Lepomis macrochirus* (Drucker and Lauder, 1999) has established that during steady swimming at $0.5\,L\,s^{-1}$ the pectoral fin wake takes the form of a toroidal vortex ring and that force components estimated independently from perpendicular laser planes are not significantly different from each other. Accordingly, we focus in this paper on wake flow patterns from a single orientation of the laser plane that maximized the image of within-plane flow during yawing turns. One video camera was used to record the movement of particles within the frontal (horizontal) plane intersecting the abducted pectoral fin at midspan, while the second camera simultaneously recorded a reference image of the posterior perspective of the fish and the laser light sheet. Synchronized signals from the two cameras were recorded separately by two S-VHS video recorders, making the entire frontal-plane video field available for quantitative flow visualization.

In this study, the shadow cast by the body of the fish made it possible to investigate wake flow patterns for the left fin only (see Fig. 1 in Drucker and Lauder, 1999). This fin was termed the 'strong-side' pectoral fin when on the same side of the body as the stimulus and the 'weak-side' fin when on the side opposite to the stimulus (see Fig. 1). Thus, by inducing both right-hand and left-hand turns in sunfish, it was possible to evaluate both the strong- and weak-side roles played by the left pectoral fin.

Kinematic and hydrodynamic measurements

Patterns of body and fin movement and of water flow in the wake were measured for each fish during turning and, for

comparison, during the immediately preceding steady fin beat at $0.5\,L\,s^{-1}$. This experimental design allowed statistical evaluation (by means of paired *t*-tests) of the degree to which steady pectoral fin swimming and unsteady pectoral fin turning differ biomechanically. From the DPIV video tapes of the four experimental fish, 26 sequences of steady swimming followed by turning were reviewed to establish general wake flow patterns. Of these sequences, nine left-hand turns, nine right-hand turns and the 18 associated steady strides were selected for detailed quantitative analysis.

Three kinematic variables were measured from DPIV video tapes. First, the duration of propulsive pectoral fin movement τ was determined. For the purpose of calculating locomotor force, τ was defined for both steady swimming and turning as the time over which the body translated or rotated as a result of pectoral fin excursions. Thus, during steady forward swimming, τ was taken as the entire period of pectoral fin oscillation. During turning, movements of the strong-side pectoral fin were associated with body rotation from the beginning of abduction to the end of adduction (Fig. 1A–E), and τ was therefore measured as the duration of the downstroke plus upstroke. The weak-side fin, in contrast, showed a variable period of prolonged, weak abduction followed by rapid and forceful adduction (Fig. 1C–E). Accordingly, τ in this case was taken as the duration of the pectoral fin upstroke. The second kinematic variable measured was the mean angular velocity of the body in the horizontal plane during yawing turns. The change in body angle over τ was determined as the degree of rotation of the midline segment between the anterior insertions of the anal fin and the pelvic fins. Finally, the average linear velocity of the body during turning was measured by tracking the displacement of the midline point of insertion of the pelvic fins. Measures of both angular and linear displacement were made from digitized video images using custom-designed image-analysis software.

Unsteady two-dimensional water velocity fields in the wake of the pectoral fin were calculated from consecutive digital images (640 pixels×480 pixels) by means of spatial cross-correlation (Willert and Gharib, 1991; Raffel et al., 1998). In total, 97 image pairs from steady swimming and turning events were processed for calculation of wake structure and strength. Frontal-plane flow fields were typically 7–9 cm on each side and made up of 20×20 matrices of velocity vectors. Post-processing of DPIV data, including the validation of velocity vectors, was performed as described previously (Drucker and Lauder, 1999). The average free-stream flow velocity was subtracted from each vector matrix to reveal vortical structures in the wake and to allow measurement of flow geometry. The distance between paired vortex cores was taken as the projected diameter of three-dimensional vortex rings shed into the wake. The mean orientation of velocity vectors in the central fluid jet of each vortex pair was measured relative to the initial heading of the fish (i.e. the longitudinal axis of the body) (see Fig. 6 in Drucker and Lauder, 2000). This jet angle was determined at the end of the upstroke, at which time paired vortices were fully developed.

The calculation of derivative and integral quantities related to flow structure and force (vorticity and circulation, respectively) was carried out as described previously (Drucker and Lauder, 1999). Fluid momentum (*M*) carried into the wake over the course of each fin stroke was computed as the product of water density, mean vortex circulation and vortex ring area. The total stroke-averaged force ($\bar{F}$) exerted by the pectoral fin on the fluid was then calculated following Milne-Thomson (Milne-Thomson, 1966) according to:

$$\bar{F} = M/\tau\,. \tag{1}$$

To assess the functional roles of the strong- and weak-side fins during turning, total momentum and force were partitioned into perpendicular components aligned with anatomical reference axes. The posterior component lay in line with the longitudinal axis of the fish at the onset of propulsive fin motion irrespective of the degree of rotation of the body relative to the incident water flow. The lateral component was oriented perpendicular to the posteriorly directed component (see Fig. 4A,B). As discussed above, the strong- and weak-side pectoral fins make propulsive excursions during different portions of the fin stroke cycle. Accordingly, the perpendicular components of *M* and $\bar{F}$ were determined according to the fish's heading at the onset of abduction of the strong-side fin and the onset of adduction of the weak-side fin.

Results

Kinematic patterns

Turning maneuvers performed by sunfish in response to the given stimulus were powered by movements of the paired pectoral fins. In contrast to the symmetrical motions of the left and right fins observed during steady labriform swimming (Gibb et al., 1994; Drucker and Lauder, 1999), yawing turns by sunfish are characterized by temporally and spatially asymmetrical excursions of the contralateral fins. A representative turning maneuver is illustrated in Fig. 1. Whether issued on the left or right side of the body, the stimulus (Fig. 1A) immediately results in rapid abduction (downstroke) of the strong-side pectoral fin (Fig. 1B). The weak-side fin exhibits a delayed onset of abduction and reaches a position of maximal abduction only after the strong-side fin begins its return stroke towards the body (Fig. 1C). During this period, the body rotates within the frontal plane towards the weak side with little or no translation. While rotation of the body continues, the weak-side fin remains in a fully abducted position and then undergoes rapid adduction (upstroke) together with the strong-side fin (Fig. 1D). At the onset of adduction of the weak-side fin, the longitudinal axis of the body completes a rotation of 25.7±4.1 ° (mean ± S.E.M., *N*=9). After this change in heading, the fish translates away from the source of the stimulus (Fig. 1E). During the turning response, therefore, early abduction of the strong-side fin is associated with body rotation, and late adduction of the weak-side fin is correlated with body translation.

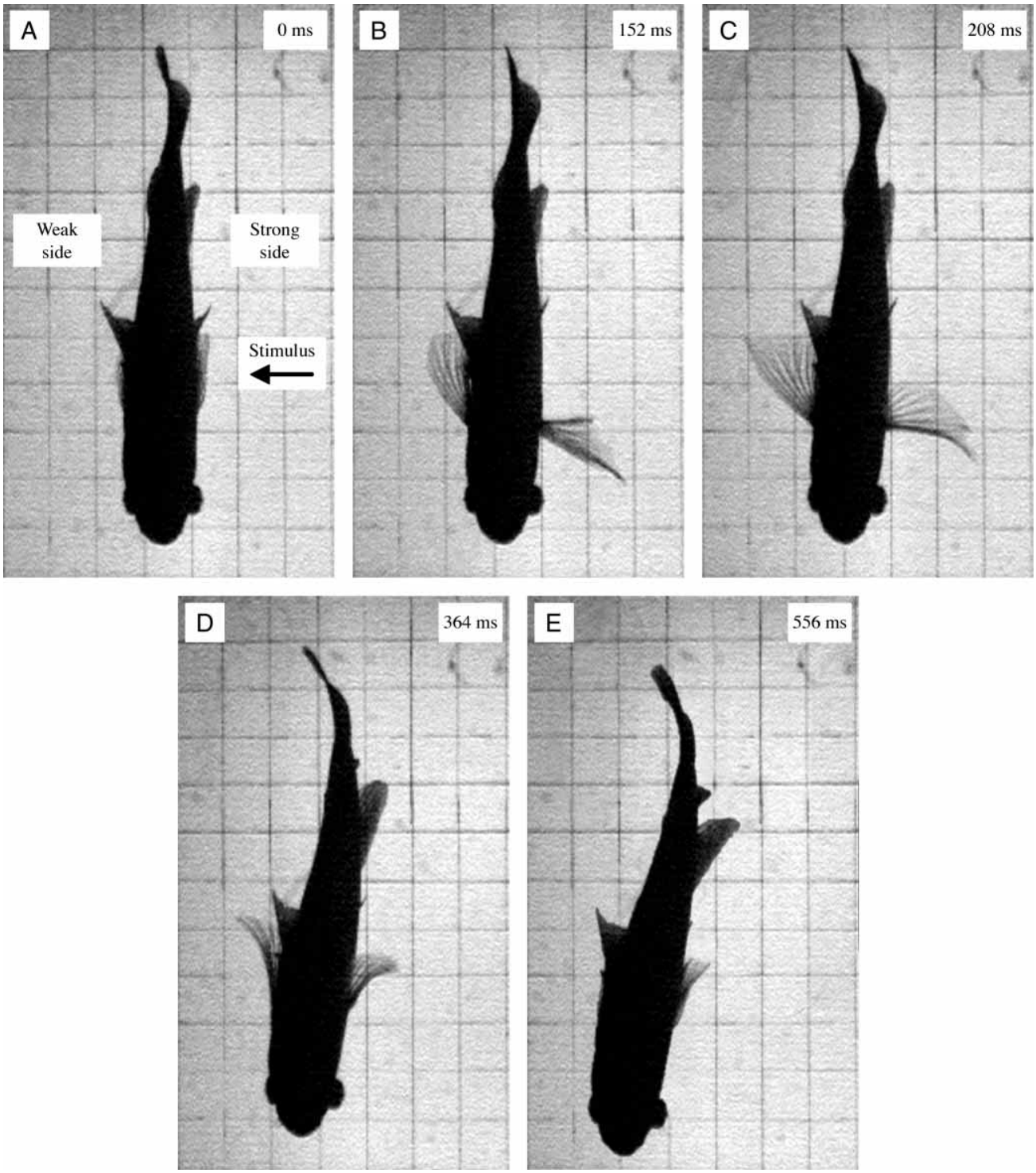

Fig. 1. Ventral silhouettes of sunfish during a representative turning maneuver performed with the pectoral fins. The fin on the same side of the body as the turning stimulus is termed the 'strong-side' fin, while the contralateral fin is termed the 'weak-side' fin. Wake flow patterns could be observed for only one pectoral fin (here pictured on the right side of each panel; see Materials and methods) and thus, during experiments, stimuli were issued on both the left and right sides of the fish to visualize the wake of this fin in its strong- and weak-side roles. (A) A fish shown swimming steadily against a current of 0.5 body length s^{-1} (11.2 cm s^{-1}) moving from the bottom to the top of the page. As the pectoral fins adduct against the body at the end of the fin beat, the stimulus is given. (B) Peak abduction of the strong-side fin; early abduction of the weak-side fin. (C) Peak abduction of the weak-side fin; early adduction of the strong-side fin. (D,E) Synchronous adduction of both fins. Note that the evasive maneuver performed by the sunfish in response to the stimulus consists of two distinct phases: body rotation (A–D) and body translation (D,E). At the end of the behavior, slight flexion of the posterior trunk and tail (D,E) is not followed by axial propulsion. The distance between background grid marks is 2 cm.

Table 1. *Wake measurements from steady swimming and turning by bluegill sunfish*

Measurement	Steady swimming	Turning: strong side	Ratio	Steady swimming	Turning: weak side	Ratio
Mean jet angle (degrees)	41.2±3.9	91.6±5.5	2.22*	45.8±6.8	0.3±4.5	0.01*
Mean jet velocity ($cm\,s^{-1}$)	7.6±0.6	13.9±2.1	1.83*	8.0±0.6	11.4±1.2	1.42*
Peak jet velocity ($cm\,s^{-1}$)	11.9±0.9	26.0±4.4	2.18*	10.2±1.1	17.5±1.7	1.72*
Momentum, lateral component ($g\,cm\,s^{-1}$)	520.8±39.6	1151.7±245.0	2.21*	478.3±78.9	–81.9±90.6‡	0.17*
Momentum, posterior component ($g\,cm\,s^{-1}$)	451.0±54.6	133.1±79.0	0.30*	480.1±62.3	913.0±180.7	1.90*
Force, lateral component (mN)	5.4±0.4	20.9±6.5	3.83*	5.3±0.8	–5.3±4.4‡	1.00*
Force, posterior component (mN)	4.7±0.6	2.1±1.3	0.44*	5.6±1.5	48.3±5.5	8.64*
Force ratio, lateral:posterior	1.18±0.09	10.05±4.15	–	1.11±0.29	0.11±0.03	–

All measurements are from frontal-plane velocity fields and are reported for the end of the upstroke as mean ± S.E.M. For each variable, N=9 pectoral fin beats performed by four individuals.

Mean jet angle is defined for each fin beat as the average orientation of velocity vectors comprising the wake's central fluid jet. Mean and peak jet velocities are taken as the average and maximum vector magnitudes.

Wake momentum and force are stroke-averaged measurements reported per fin. The lateral and posterior components of these quantities are defined in Figs 3 and 4.

Ratio is the absolute value of the measurement for turning expressed as a proportion of that for steady swimming.

Measurements for steady swimming at 0.5 body length s^{-1} and for subsequent turning were compared statistically using paired t-tests (d.f.=8). Asterisks indicate significant differences at the Bonferroni-adjusted α=0.0062. Unpaired t-tests (d.f.=16) revealed no significant differences among steady fin beats preceding strong-side and weak-side turns.

‡Negative values indicate that these vector quantities are, on average, oriented medially relative to the longitudinal axis of the fish at the onset of propulsive fin movement.

The relatively large variation around some means reflects the pooling of measurements from several turns of different velocity (see Figs 3 and 4).

Wake flow patterns

Patterns of water movement in the wake of the pectoral fin are illustrated for paired observations of steady swimming and subsequent turning in Fig. 2. As reported previously for sunfish (Drucker and Lauder, 1999; Drucker and Lauder, 2000), planar visualizations of the pectoral fin wake produced by steady swimming reveal paired counterrotating vortices with central fluid jets (Fig. 2A,C). These vortices represent sections through a three-dimensional vortex ring; see Drucker and Lauder, 1999; Drucker and Lauder, 2000 for details of the dynamics of ring production and of vortex dimensions and circulation. At the relatively low swimming speed of $0.5\,L\,s^{-1}$, the ring's momentum jet is oriented obliquely downstream (mean frontal-plane jet angle ϕ measured relative to the axis of incident flow ranges between 41 and 46 °, Table 1). The velocity vectors comprising the jet generated during steady swimming have an average magnitude of $8\,cm\,s^{-1}$ and a mean maximal magnitude of 10–12 $cm\,s^{-1}$ (Table 1).

Turning maneuvers result in a pronounced reorganization of the wake patterns observed during steady swimming. In its strong-side turning role, the pectoral fin generates paired vortices during each downstroke–upstroke cycle that are substantially larger and stronger than those generated during steady swimming (Fig. 2B). The central jet is oriented primarily laterally (mean ϕ=92 °, Table 1) and is characterized by flow speeds approximately twice as great as those measured for steady swimming (Table 1). When playing its weak-side role in turning, the pectoral fin shows a variable period of slow abduction, during which little organized wake flow is developed, and upon the upstroke produces a paired-vortex wake (Fig. 2D). The central momentum flow associated with these vortices is oriented approximately in line with the anteroposterior axis of the body (at the end of fin upstroke, mean $\phi\approx$0 °, Table 1). Maximal flow velocities in the weak-side jet on average exceed those measured for steady swimming by a factor of 1.4 (Table 1). Thus, the pectoral fin is capable of producing wake flows during turning that differ radically in both orientation and velocity from those produced during constant-speed, rectilinear locomotion.

Locomotor force

Two variables related to locomotor force – vortex ring momentum and fin stroke timing (equation 1) – were measured for turning events performed by sunfish. In the initial stage of a turning maneuver, the strong-side fin generates a momentum flow whose magnitude and orientation were measured at the end of the upstroke. This vector quantity, representing the mean force impulse generated over the duration of the fin stroke, was resolved into perpendicular components aligned along anatomical body axes (Fig. 3A). In turns ranging widely in the speed of rotation of the body (2–32 ° s^{-1}), the posteriorly or backward-directed component of fluid momentum remained approximately constant (133±79 $g\,cm\,s^{-1}$, mean ± S.E.M., N=9; least-squares linear regression coefficient not significantly different from zero, P=0.50) (Fig. 3B). In contrast, the laterally or sideways-oriented component showed a significant positive association with angular velocity of the body (r^2=0.97, P<0.001) (Fig. 3B). During the rotational phase of the turning

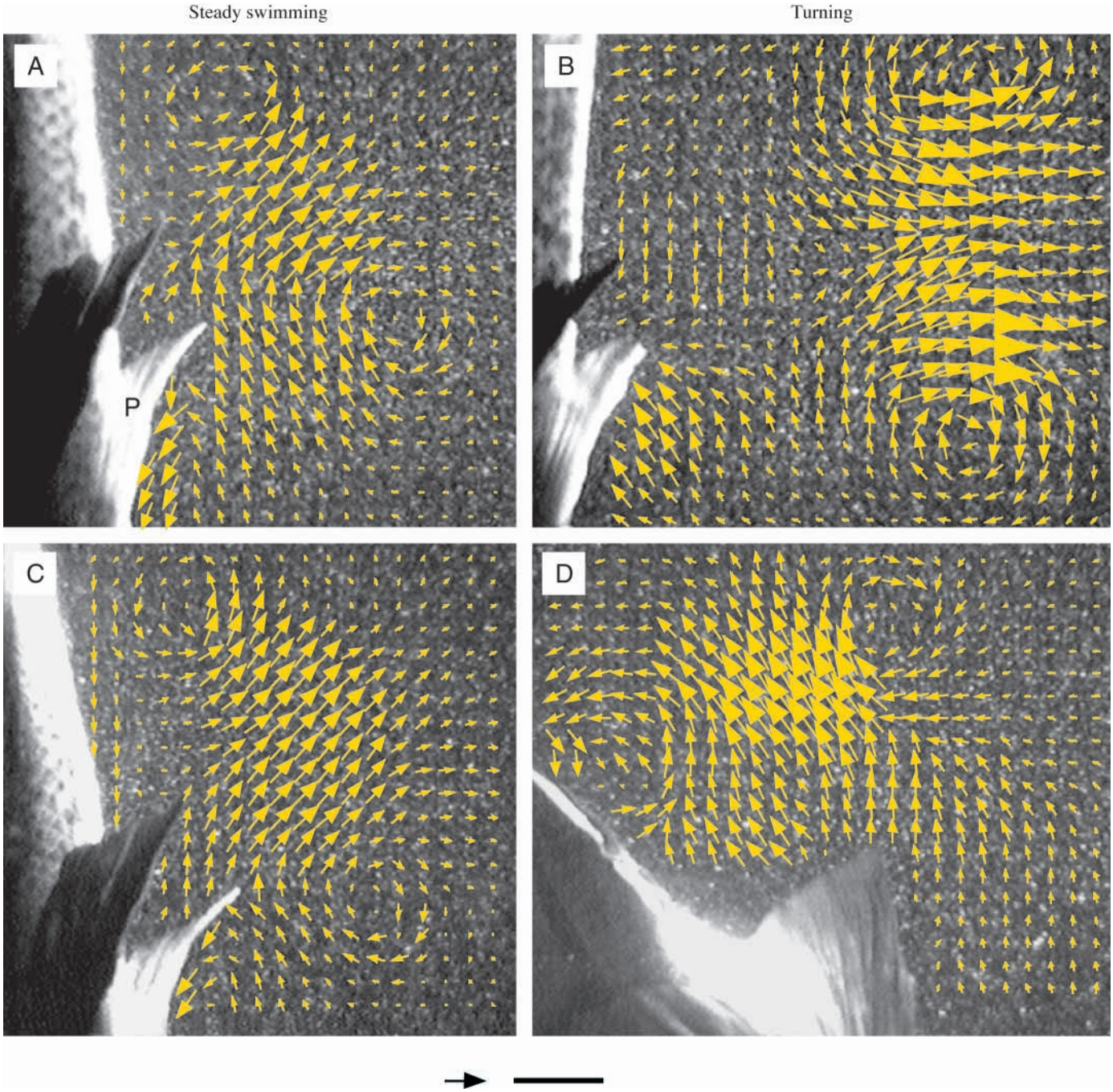

Fig. 2. Representative frontal-plane wake flow patterns during steady swimming and turning maneuvers in sunfish. For all panels, flow within the horizontal plane of analysis is shown at the final stage of the upstroke of the pectoral fin (labeled 'P'). Free-stream velocity ($0.5\,L\,s^{-1}$ or $11.2\,cm\,s^{-1}$, where L is total body length) from the bottom to the top of the page has been subtracted from each velocity vector to reveal vortical wake structures. (A) Typical pattern of fluid flow in the wake of the fin during steady swimming at $0.5\,L\,s^{-1}$ (see also Drucker and Lauder, 1999). (B) Wake flow produced by the immediately following cycle of fin downstroke and upstroke during which the fish responds to a stimulus issued from the right. As the strong-side wake develops, the body rotates in the opposite direction (cf. body position shown in Fig. 1D). (C) The wake shed by the pectoral fin during a separate instance of steady swimming. (D) The wake generated by the subsequent fin beat in response to a stimulus issued from the left. The weak-side wake depicted arises on the upstroke. The reaction to this momentum flow causes the fish to translate upstream (towards the bottom of the page) away from the source of the stimulus (the stage of the turn illustrated is comparable to that shown in Fig. 1E). Although wake flow during steady swimming shows little variation in gross form among fin beats (A,C), conspicuous differences exist in the orientation of the central jet flow in the strong-side (B) and weak-side (D) wakes. Scales: arrow, $10\,cm\,s^{-1}$; bar, 1 cm.

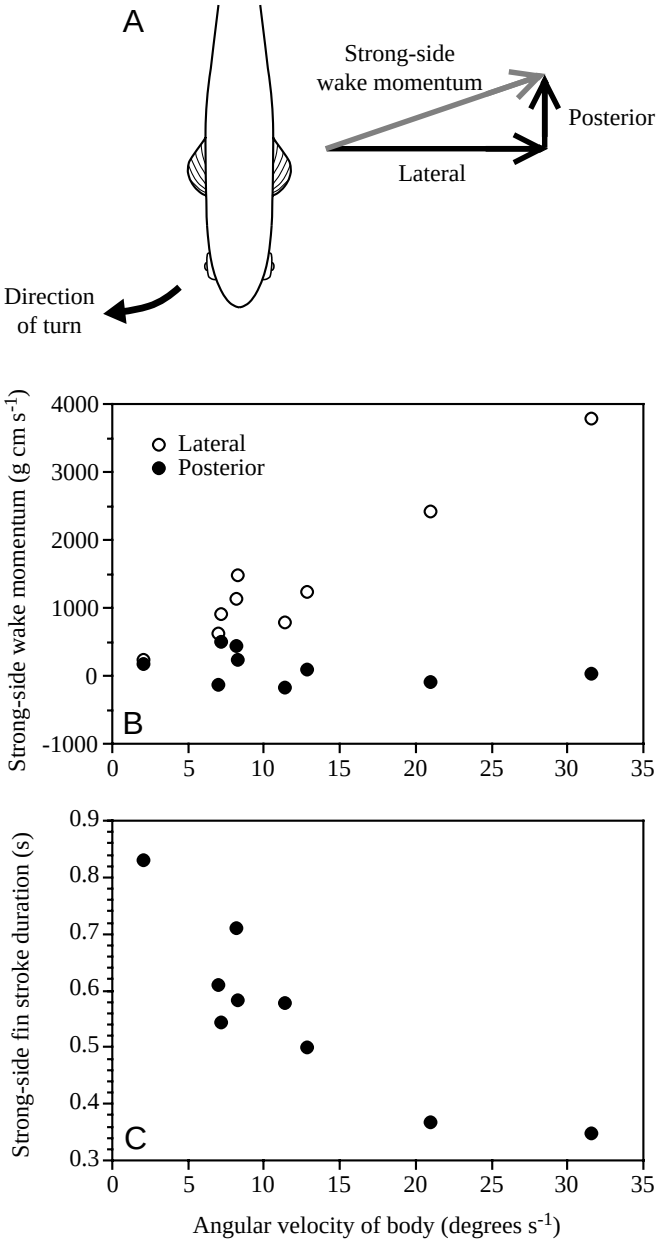

Fig. 3. Wake momentum and stroke timing for the strong-side pectoral fin during nine turning maneuvers varying in angular velocity of the body. (A) The position of the fish's body at the onset of a turn; the curved arrow indicates the direction of body rotation produced by the strong-side fin. The gray arrow represents the mean momentum flow associated with a vortex ring developed over the course of the complete fin beat (cf. Fig. 2B). Stroke-averaged momentum is resolved into laterally and posteriorly directed components (note that the magnitude of the posterior component is exaggerated for clarity); these components are regressed against the velocity of rotation of the body during turning (B). Whereas the lateral component of momentum is positively associated with the speed of rotation, the posterior component remains near zero for all turns. Positive and negative values of the posterior component of momentum signify posteriorly and anteriorly oriented jet flow, respectively. (C) The duration of the strong-side fin stroke is inversely related to the angular velocity of the body during turning. Data are from 2–3 turns performed by each of four individuals.

maneuver, lateral wake momentum exceeded that measured for steady swimming by a factor of 2.2, while posteriorly oriented momentum was approximately 30 % of that for steady locomotion (Table 1). The time period over which momentum was transferred into the wake by the fin declined sharply with increasing rotational velocity of the body in the sample of strong-side turns studied (Fig. 3C). For all turns examined in this study, the duration of propulsive motion of the strong-side fin was less than the average stroke period measured for steady swimming (0.98±0.03 s, mean ± S.E.M., N=18).

To evaluate the functional roles of the pectoral fins during turning, it was necessary to analyze the magnitude and orientation of wake forces generated on the strong and weak sides of the body (Fig. 4). Locomotor force exerted by the strong-side fin arises at the onset of the downstroke. This force shows a relationship to turning speed which mirrors that observed for strong-side wake momentum: the lateral component increases directly with the angular velocity of the rotating body, whereas the posterior component remains near zero (2.1±1.3 mN, mean ± S.E.M., N=9; regression coefficient not significantly different from zero, P=0.50) (Fig. 4C). The upstroke of the weak-side fin initiates body translation and, accordingly, weak-side forces were regressed against the linear, rather than the angular, velocity of the body. For the weak-side fin, the relationship between turning forces and body speed is opposite to that for the strong-side fin. Namely, the posteriorly oriented component of force rises with increasing velocity of the body, and the laterally directed component is of relatively low magnitude across all speeds (–5.3±4.4 mN, mean ± S.E.M., N=9; regression coefficient not significantly different from zero, P=0.15) (Fig. 4D). During turning maneuvers, the lateral force developed by the strong-side fin and the posterior force developed by the weak-side fin exceed by fourfold and ninefold, respectively, the corresponding mean values observed during steady swimming (Table 1).

Variables related to the mechanism of propulsion are summarized graphically in Fig. 5 for both steady swimming and turning. For all kinematic and hydrodynamic variables measured, no significant differences were detected among steady fin beats at $0.5\,L\,s^{-1}$ (unpaired t-tests between steady beats preceding strong- and weak-side turns, d.f.=16; P=0.19–0.96). In contrast, these variables (with the exception of mean and peak jet velocity, Table 1) differed significantly between turns towards the strong and weak sides of the body (unpaired t-tests, d.f.=16; P<0.01). For all variables, significant differences were also observed between steady fin beats and immediately following turning events (Table 1; paired t-tests, d.f.=8; P<0.01). For example, the duration of propulsive fin movement during turning is on average 0.43–0.82 s shorter than during prior steady swimming (Fig. 5A). In addition, the momentum jet produced during turning maneuvers is offset from the mean jet angle measured during rectilinear locomotion by +48.2 ° for the strong-side fin and –45.6 ° for the weak-side fin (Fig. 5B). Associated with these kinematic and geometric differences is a notable disparity in the resultant

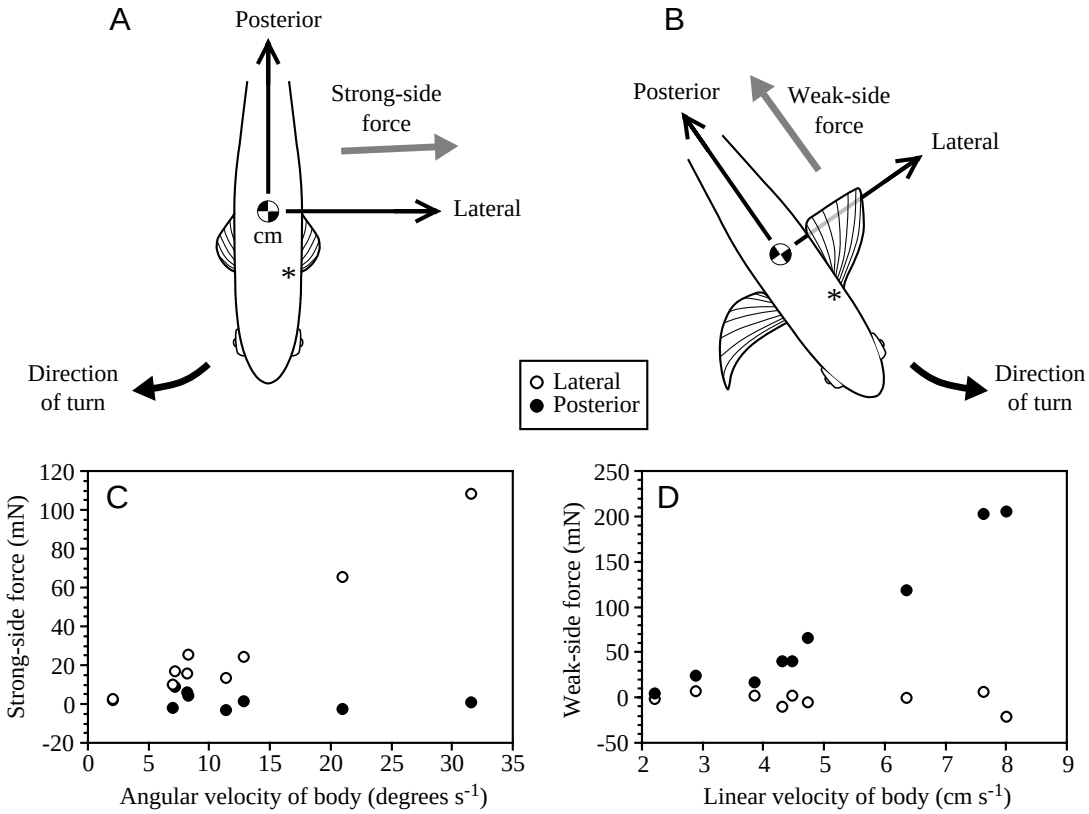

Fig. 4. Stroke-averaged forces exerted by the pectoral fin during turning maneuvers. (A,B) Drawings depicting turns in opposite directions to illustrate the strong- and weak-side roles played by a pectoral fin on one side of the body. Lateral and posterior body axes are shown at the onset of the strong-side fin downstroke (A) (cf. Fig. 1A) and at the onset of the weak-side fin upstroke (B) (cf. Fig. 1C). Gray arrows represent schematically in both cases the orientation of total wake-derived force at the end of the complete fin stroke (cf. Fig. 2B,D). Total force was resolved into perpendicular components aligned with body axes at the onset of propulsive fin motion. Note the positive association (C) between force directed laterally by the strong-side fin and the angular velocity of the body during turning, and (D) between force directed posteriorly by the weak-side fin and the linear velocity of the body during turning. Positive and negative values of the posterior component indicate, respectively, posteriorly and anteriorly directed forces, and positive and negative values of the lateral component indicate laterally and medially oriented forces. The posterior component of force for the strong-side fin (C) and the lateral component of force for the weak-side fin (D) remain near zero for all turns examined. For both C and D, the data plotted are from 2–3 turns performed by each of four individuals. Reaction forces are exerted on the fish's body at the point of insertion of the pectoral fin (marked by an asterisk). cm, approximate location of the center of mass of the body (based on Webb and Weihs, 1994).

fluid force generated by the two behaviors: turning involves total mean locomotor forces that exceed those of steady swimming by 14–42 mN per stroke (Fig. 5C).

Discussion

Mechanism of turning

Turning manuevers by fishes encompass a broad range of locomotor behaviors involving a variety of propulsors. At one extreme, fishes are capable of extremely rapid escape turning driven by Mauthner-cell-mediated body flexion (Eaton et al., 1977; Eaton et al., 1988; Eaton and DiDomenico, 1986). Such 'startle response' or 'fast-start' turns are characterized by linear accelerations of the body from rest up to 100–245 m s^{-2} and maximum angular velocities of body rotation of the order of 60 rad s^{-1} (Harper and Blake, 1990; Domenici and Blake, 1991; Kasapi et al., 1993; for reviews, see Blake, 1983; Webb and Blake, 1985). 'Cruising turns' of intermediate speed (9–17 rad s^{-1}) may alternatively be accomplished over multiple strides by steering the body in a curved trajectory with the median and paired fins or caudal fin propeller (Gerstner, 1999). The maneuvers elicited here in sunfish, representing a further class of turning behavior, are submaximal responses to an external stimulus that are characterized by turning rates not exceeding 32 ° s^{-1} (Fig. 3) or 0.6 rad s^{-1}. Such turns are powered by pectoral fin oscillation as opposed to body and caudal fin undulation and involve an initial body rotation with minimal translation, and a subsequent body translation that defines the trajectory of the animal away from the source of the stimulus. These unsteady yet relatively slow modifications of body position are accomplished within a single stride (Fig. 1).

To change its heading in this way, an animal must generate an imbalance of locomotor forces on opposite sides of the

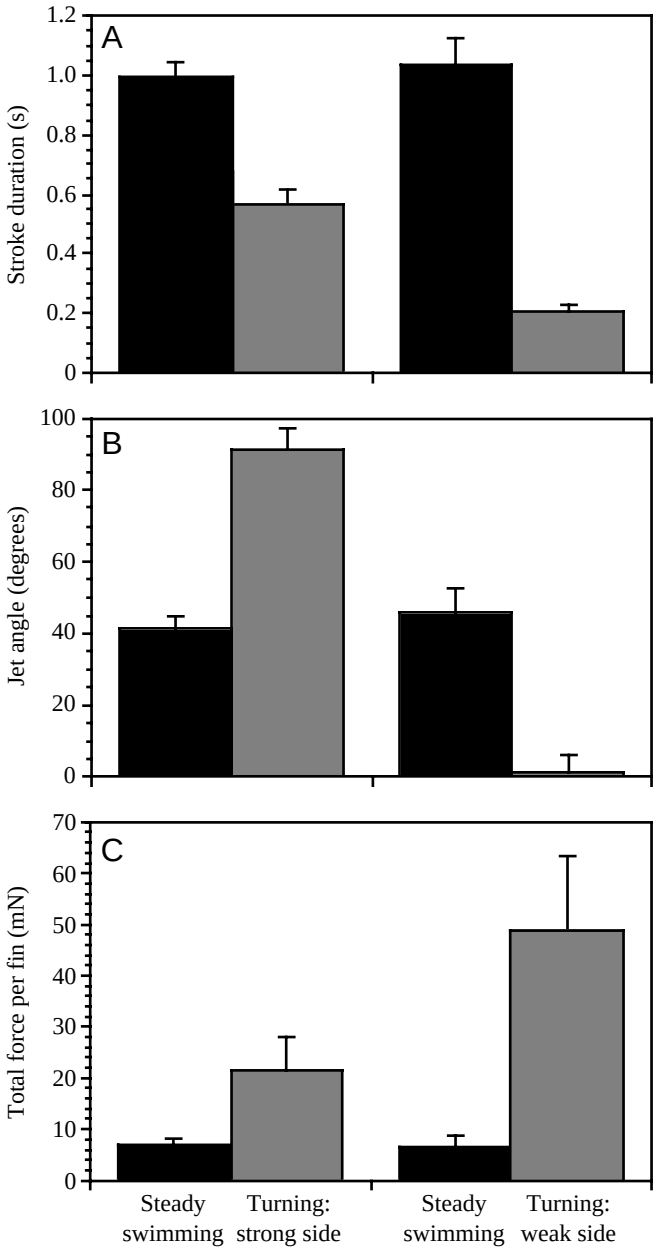

Fig. 5. Kinematic and hydrodynamic variables measured during steady swimming and turning by sunfish. Black columns represent measurements from two separate groups of fin beats during steady swimming at $0.5\,L\,s^{-1}$, where L is total body length. Gray columns signify measurements for the strong- and weak-side fins during turning maneuvers that immediately followed steady swimming fin beats. Values are presented as mean + S.E.M. (N=9 fin beats for each category). Paired t-tests reveal significant differences between steady swimming and turning in (A) the duration of propulsive pectoral fin movement, (B) the orientation of the wake's momentum jet, and (C) the total locomotor force applied to the fluid by each fin over the course of the stroke. See text for discussion.

body. In sunfish, asymmetrical forces are applied to the fluid both through a temporal delay between movements of the strong- and weak-side pectoral fins and through pronounced variation in contralateral wake geometry. Early abduction of the strong-side fin (Fig. 1B) results in a laterally oriented jet flow (Fig. 2B) that is largely unopposed by the wake of the slowly moving weak-side fin. More rapid rotations of the body during turning are associated with larger laterally oriented momentum flows in the wake and shorter periods of fin movement (Fig. 3). Sunfish are therefore capable of modulating both vortex ring impulse and the timing of wake production in order to control the fluid forces of turning (see equation 1).

In this study, quantification of turning moments around the center of mass of the body was precluded by the experimental requirements of DPIV image recording. To visualize details of the pectoral fin wake, we used a relatively high-magnification field of view that included the laser-illuminated flow field but excluded much of the body of the fish (Fig. 2). As a result, it was not possible to measure directly the location of the center of mass of the body from DPIV video images, and thus calculation of moment arms for turning (i.e. the perpendicular distance between the center of mass and the line of action of the reaction force acting on the fish) was not attempted. However, the functional roles of the strong- and weak-side pectoral fins in turning can be assessed qualitatively in terms of the location and orientation of reaction forces acting on the body. Fluid forces exerted on the surface of the pectoral fin are transmitted to the body through the fin base (marked with asterisks in Fig. 4A,B). For the fish examined in this study, the fin base is located 5.0±0.1 cm (mean ± S.D., N=4) posterior to the snout, a longitudinal position corresponding to 24±1 % of body length L. Webb and Weihs report that the center of mass of adult *Lepomis macrochirus* is situated, on average, 2.9 cm further posteriorly at 0.36L (Webb and Weihs, 1994). The large medially directed forces on the fin base arising in reaction to the laterally directed strong-side forces applied to the fluid (Fig. 4C) are therefore located to generate torque around the center of mass. Accordingly, we conclude that the primary role of the strong-side fin in turning is to change the fish's heading by rotating the body. In contrast, the large anteriorly directed reaction forces acting on the opposite side of the body (Fig. 4D) support a primary role of body translation for the weak-side pectoral fin. The absence of pronounced side-slip during the rotational phase of the turn in bluegill sunfish may reflect a stabilizing influence of body depth. Other fishes that are not as deep-bodied should be more susceptible to lateral displacement of the center of mass during rotation arising in reaction to the strong-side fin's momentum jet.

The mechanism by which fishes turn with the paired fins has been the subject of limited experimental study. On the basis of qualitative observations of swimming kinematics, Breder proposed two strategies for changing body orientation by means of the pectoral fins: (i) suspending weak-side fin motion while continuing strong-side fin motion, as during steady swimming; and (ii) suspending strong-side fin motion while holding the weak-side fin in an abducted position to function as a pivot (Breder, 1926). The applicability of these turning mechanisms is far from universal among bony fishes, and their distribution instead appears to be related to the primary

strategy employed for rectilinear locomotion. For example, the first mechanism has been documented for balistiform swimmers (Blake, 1978) and the second for fishes that swim by axial undulation (Harris, 1936) or tetraodontiform locomotion (Breder, 1926).

In the labriform swimmer *Lepomis macrochirus*, however, pectoral fin turning is accomplished by a considerably more complex method. At no time during turning is pectoral fin motion unilaterally suspended by *Lepomis macrochirus*. Although the weak-side fin does initially undergo prolonged abduction, suggesting a secondary role as a drag-based pivot (Fig. 1B,C), the strong-side fin exhibits motions during turning that are distinct from those observed during steady swimming. Similar patterns have been observed for the living crossopterygian fish *Latimeria chalumnae*, which uses pectoral fin locomotion to swim in open water (Fricke et al., 1987; Fricke and Hissmann, 1992). The coelacanth initiates swimming along a curved trajectory by strokes of the strong-side pectoral fin, while simultaneously abducting the weak-side fin to achieve a 'braking' effect. Subsequent simultaneous adduction of both fins results in forward translation of the body (cf. Fig. 1).

We conclude that the two mechanisms proposed by Breder (Breder, 1926) provide an incomplete description of turning maneuvers for fishes that rely primarily on the pectoral fins for propulsion. For such fishes, changes in heading can be achieved in a limited space by body rotation without translation (see also Gerstner, 1999) and, in general, involve synchronous but asymmetrical fin movements. Our data show that the hydrodynamic hallmark of slow pectoral fin turning, as elicited in bluegill sunfish, is the marked variation in wake flow orientation between the contralateral pectoral fins (Fig. 2B,D). In addition, as suggested by Breder (Breder, 1926) and Harris (Harris, 1936), the dorsal, anal and caudal fins may also play central roles in turning. Analysis of the hydrodynamic function of these median fins will be an important next step in understanding the biomechanical basis of maneuvering in fishes.

Comparisons with steady locomotion

The first hypothesis of Breder argues that turning is a relatively minor functional modification of steady swimming (i.e. turning is accomplished by performing rectilinear locomotion unilaterally) (Breder, 1926). For bluegill sunfish, however, steady swimming and turning are biomechanically distinct behaviors, differing at three levels of analysis: fin kinematics, wake structure and momentum, and locomotor force. First, straight-ahead locomotion and turning involve different spatial and temporal patterns of pectoral fin movement. For fish of the size examined in this study swimming at $0.5\,L\,s^{-1}$, rectilinear swimming is characterized by synchronous beating of the left and right fins at approximately 1 Hz (Gibb et al., 1994; Drucker and Lauder, 1999). Turning involves asymmetrical left–right fin motions (Fig. 1) that are significantly shorter in duration than those observed during steady swimming (Fig. 5A). Second, the two behaviors generate momentum flows in the wake that differ radically in orientation. While the vortex ring's jet remains at nearly 45° to the body on average during steady swimming (Table 1; Fig. 2A,C), momentum flows during turning are directed approximately perpendicular and parallel to the longitudinal axis of the body by the strong-side and weak-side fins, respectively (Table 1; Figs 2B,D, 5B). The magnitude of the wake momentum also varies between the behaviors: the strong- and weak-side fins, respectively, generate lateral and posterior force impulses during turning that exceed those produced during rectilinear locomotion by a factor of 1.9–2.2 (Table 1). Third, the total wake forces produced by steady fin beats and turning maneuvers show pronounced differences in magnitude. The resultant wake force (i.e. the geometric resolution of laterally and posteriorly oriented force components) is 3–7 times greater during turning events than during preceding cycles of straight-ahead locomotion at $0.5\,L\,s^{-1}$ (Fig. 5C). These mechanistic differences demonstrate that turning with the paired fins is not simply steady swimming performed unilaterally.

A comparative analysis of locomotor force, in particular, highlights the pronounced mechanistic variation that exists among pectoral fin swimming behaviors. Previous work (Drucker and Lauder, 1999; Drucker and Lauder, 2000) on steadily swimming bluegill sunfish showed that total pectoral fin thrust increases with swimming speed and reaches a maximum at the speed of recruitment of axial undulation. Above this gait transition speed, pectoral fin force plateaus, suggesting a potential limit to the rate at which momentum can be added to the wake. In addition, across all speeds studied, the sunfish maintains an approximately constant ratio (mean 1.13) of laterally to downstream-directed force components. The present study of unsteady maneuvering demonstrates that the relatively invariant mechanism used for steady swimming does not accurately represent the pectoral fin's complete range of function. During turning, for example, the posterior component of weak-side force (Table 1, 48.3 mN) exceeds the maximum thrust forces measured at the fastest speed of steady pectoral fin swimming by a factor of 2–3. Furthermore, the ratio of lateral to posterior force measured for turning spans almost two orders of magnitude: whereas this ratio is near unity for steady swimming, it rises by a factor of 9 for the strong-side fin (to 10.0) and falls by a factor of 10 for the weak-side fin (to 0.11; Table 1). These observations, revealed by experimental analysis of turning maneuvers, underscore the enormous functional versatility of the teleost pectoral fin.

The extent to which steady locomotion and maneuvering differ biomechanically is also interesting from the perspective of neuromuscular control. Recent work by Jindrich and Full revealed that for a terrestrial arthropod (the cockroach *Blaberus discoidalis*), turning can arise from minor adjustments to the mechanism used for straight-ahead running (Jindrich and Full, 1999). The stride frequency and gait used by cockroaches during rectilinear locomotion did not change during turning, and only subtle differences between the behaviors were observed in the orientation and magnitude of

force impulses applied by the legs. On the basis of these similarities, Jindrich and Full proposed that the dynamically stable, sprawled posture of many-legged insect runners may simplify the neuromuscular control of a wide range of locomotor behaviors (Jindrich and Full, 1999). In vertebrates, more complex control mechanisms may allow radical changes in behavior between steady and unsteady locomotion, as observed here for *Lepomis macrochirus*. Whether the complexity of the control system is correlated with the breadth of the behavioral repertoire, however, is a question that awaits future research.

Quantifying maneuverability

Defining maneuverability in terms of a measurable quantity is a critical prerequisite for the comparative study of unsteady locomotor performance. The most useful quantitative index of maneuverability would be applicable to animals that move both on land and through fluid, irrespective of locomotor mode. Such an index may be defined either kinematically, to provide a numerical descriptor of unsteady body motion, or in terms of the locomotor forces generated, to reflect the mechanism underlying maneuverability. In previous studies of maneuverability in fishes (e.g. Howland, 1974; Webb, 1983; Gerstner, 1999), turning performance has been evaluated kinematically in terms of the minimum turning radius as measured from trajectories of the center of mass of the body. A recently proposed force-based index is the linear maneuverability number (LMN) (Jindrich and Full, 1999). The LMN measures the force impulse exerted by a propulsor in a direction perpendicular to the animal's heading as a proportion of the forward momentum of the animal's center of mass. The force impulse is defined as the component of force perpendicular to the heading integrated over the stride period. In this study, we approximated the index for turns performed by sunfish according to:

$$\mathrm{LMN} \approx M_{\perp}/mU, \qquad (2)$$

where $M_{\perp}$ is the stroke-averaged wake momentum oriented perpendicular to the fish's initial heading (i.e. before body rotation) produced by the strong-side fin (see Table 1, lateral component of momentum), m is the body mass in air and U is the forward velocity of the body before the turn. In effect, the LMN reflects the ability of an animal to generate laterally oriented momentum in order to deflect its own forward progress. For the turns examined in this study, LMN ranged from 0.12 to 0.74, indicating that sunfish are able to generate approximately one-tenth to three-quarters of their own forward momentum as laterally oriented wake momentum. In their study of hexapedal locomotion, Jindrich and Full found that cockroaches turn with a mean LMN of 0.75 (Jindrich and Full, 1999). The primary benefit of the LMN as a measure of maneuvering performance is that its calculation does not depend directly upon the specific kinematics of any given locomotor system and it can therefore serve as an index for cross-taxonomic comparisons (such as the sunfish–cockroach comparison above). An additional advantage of the LMN is that it is based upon empirically determined force impulses produced by a maneuvering animal rather than indirect or theoretical estimates of momentum.

On the basis of large laterally oriented wake forces produced during steady swimming, Drucker and Lauder predicted that the bluegill sunfish should be capable of a turning performance superior to that of species exerting lower lateral forces during straight-ahead swimming (Drucker and Lauder, 2000). As reflected by the LMN calculated for the fastest turns, sunfish are indeed capable of relatively high maneuverability. However, this study also demonstrates that the ratio of laterally to posteriorly directed force measured during steady swimming can be substantially altered during turning maneuvers. Depending on which side of the body is under consideration, this ratio can rise or fall by nearly an order of magnitude (Table 1). Therefore, predictions about maneuverability based upon steady swimming forces must be considered tentative. Additional study is required to evaluate the extent to which unsteady maneuvering ability in fishes is achieved at the expense of steady locomotor performance.

Support from NSF (DBI-9750321 to E.G.D. and IBN-9807012 to G.V.L.), the comments of two anonymous reviewers and assistance provided by Jimmy Liao, Jen Nauen and Cheryl Wilga are gratefully acknowledged.

References

Aldridge, H. D. J. N. (1987). Turning flight of bats. *J. Exp. Biol.* **128**, 419–425.

Arnold, G. P., Webb, P. W. and Holford, B. H. (1991). The role of the pectoral fins in station-holding of Atlantic salmon parr (*Salmo salar* L.). *J. Exp. Biol.* **156**, 625–629.

Blake, R. W. (1978). On balistiform locomotion. *J. Mar. Biol. Ass. U.K.* **58**, 73–80.

Blake, R. W. (1979). The energetics of hovering in the mandarin fish (*Synchropus picturatus*). *J. Exp. Biol.* **82**, 25–33.

Blake, R. W. (1983). *Fish Locomotion*. Cambridge: Cambridge University Press.

Blake, R. W., Chatters, L. M. and Domenici, P. (1995). Turning radius of yellowfin tuna (*Thunnus albacares*) in unsteady swimming manoeuvres. *J. Fish Biol.* **46**, 536–538.

Breder, C. M., Jr (1926). The locomotion of fishes. *Zoologica* **4**, 159–296.

Dickinson, M., Farley, C. T., Full, R. J., Koehl, M. A. R., Kram, R. and Lehman, S. (2000). How animals move: an integrative view. *Science* **288**, 100–106.

Domenici, P. and Blake, R. W. (1991). The kinematics and performance of the escape response in the angelfish (*Pterophyllum eimekei*). *J. Exp. Biol.* **156**, 187–205.

Domenici, P. and Blake, R. W. (1997). The kinematics and performance of fish fast-start swimming. *J. Exp. Biol.* **200**, 1165–1178.

Drucker, E. G. and Lauder, G. V. (1999). Locomotor forces on a swimming fish: three-dimensional vortex wake dynamics quantified using digital particle image velocimetry. *J. Exp. Biol.* **202**, 2393–2412.

Drucker, E. G. and Lauder, G. V. (2000). A hydrodynamic analysis

of fish swimming speed: wake structure and locomotor force in slow and fast labriform swimmers. *J. Exp. Biol.* **203**, 2379–2393.

Eaton, R. C., Bombardieri, R. A. and Meyer, D. (1977). The Mauthner initiated startle response in teleost fish. *J. Exp. Biol.* **66**, 65–81.

Eaton, R. C. and DiDomenico, R. (1986). Role of the teleost escape response during development. *Trans. Am. Fish. Soc.* **115**, 128–142.

Eaton, R. C., DiDomenico, R. and Nissanov, J. (1988). Flexible body dynamics of the goldfish C-start: implications for reticulospinal command mechanisms. *J. Neurosci.* **8**, 2758–2768.

Eilam, D. (1994). Influence of body morphology on turning behavior in carnivores. *J. Motor Behav.* **26**, 3–12.

Fricke, H. and Hissmann, K. (1992). Locomotion, fin coordination and body form of the living coelacanth *Latimeria chalumnae*. *Env. Biol. Fish.* **34**, 329–356.

Fricke, H., Reinicke, O., Hofer, H. and Nachtigall, W. (1987). Locomotion of the coelacanth *Latimeria chalumnae* in its natural environment. *Nature* **329**, 331–333.

Fuiman, L. A. and Webb, P. W. (1988). Ontogeny of routine swimming activity and performance in zebra danios (Teleostei: Cyprinidae). *Anim. Behav.* **36**, 250–261.

Geerlink, P. J. (1987). The role of the pectoral fins in braking of mackerel, cod and saithe. *Neth. J. Zool.* **37**, 81–104.

Gerstner, C. L. (1999). Maneuverability of four species of coral-reef fish that differ in body and pectoral-fin morphology. *Can. J. Zool.* **77**, 1102–1110.

Gibb, A. C., Jayne, B. C. and Lauder, G. V. (1994). Kinematics of pectoral fin locomotion in the bluegill sunfish *Lepomis macrochirus*. *J. Exp. Biol.* **189**, 133–161.

Gray, J. (1933). Directional control of fish movement. *Proc. R. Soc. Lond. B* **113**, 115–125.

Harper, D. G. and Blake, R. W. (1990). Fast-start performance of rainbow trout *Salmo gairdneri* and northern pike *Esox lucius*. *J. Exp. Biol.* **150**, 321–342.

Harris, J. E. (1936). The role of the fins in the equilibrium of the swimming fish. I. Wind tunnel tests on a model of *Mustelus canis* (Mitchell). *J. Exp. Biol.* **13**, 476–493.

Harris, J. E. (1937). The mechanical significance of the position and movements of the paired fins in the Teleostei. *Pap. Tortugas Lab.* **31**, 173–189.

Harris, J. E. (1938). The role of the fins in the equilibrium of the swimming fish. II. The role of the pelvic fins. *J. Exp. Biol.* **16**, 32–47.

Howland, H. C. (1974). Optimal strategies for predator avoidance: the relative importance of speed and manoeuvrability. *J. Theor. Biol.* **47**, 333–350.

Jindrich, D. L. and Full, R. J. (1999). Many-legged maneuverability: dynamics of turning in hexapods. *J. Exp. Biol.* **202**, 1603–1623.

Kasapi, M. A., Domenici, P., Blake, R. W. and Harper, D. (1993). The kinematics and performance of escape responses of the knifefish *Xenomystus nigri*. *Can. J. Zool.* **71**, 189–195.

Kato, N. (1998). Locomotion by mechanical pectoral fins. *J. Mar. Sci. Technol.* **3**, 113–121.

Kato, N. (1999). Hydrodynamic characteristics of a mechanical pectoral fin. *J. Fluids Eng.* **121**, 605–613.

Kato, N. and Furushima, M. (1996). Pectoral fin model for maneuver of underwater vehicles. *Proceedings of the 1996 IEEE Symposium on Autonomous Underwater Vehicle Technology* **3**, 113–121.

Lauder, G. V. (2000). Function of the caudal fin during locomotion in fishes: kinematics, flow visualization, and evolutionary patterns. *Am. Zool.* **40**, 101–122.

Milne-Thomson, L. M. (1966). *Theoretical Aerodynamics*, fourth edition. New York: Macmillan.

Müller, U. K., Stamhuis, E. J. and Videler, J. J. (2000). Hydrodynamics of unsteady fish swimming and the effects of body size: comparing the flow fields of fish larvae and adults. *J. Exp. Biol.* **203**, 193–206.

Müller, U. K., Van den Heuvel, B. L. E., Stamhuis, E. J. and Videler, J. J. (1997). Fish foot prints: morphology and energetics of the wake behind a continuously swimming mullet (*Chelon labrosus* Risso). *J. Exp. Biol.* **200**, 2893–2906.

Raffel, M., Willert, C. E. and Kompenhans, J. (1998). *Particle Image Velocimetry: A Practical Guide*. Heidelberg: Springer-Verlag.

Schrank, A. J. and Webb, P. W. (1998). Do body and fin form affect the abilities of fish to stabilize swimming during maneuvers through vertical and horizontal tubes? *Env. Biol. Fish.* **53**, 365–371.

Warrick, D. R. (1998). The turning- and linear-maneuvering performance of birds: the cost of efficiency for coursing insectivores. *Can. J. Zool.* **76**, 1063–1079.

Webb, P. W. (1983). Speed, acceleration and manoeuvrability of two teleost fishes. *J. Exp. Biol.* **102**, 115–122.

Webb, P. W. (1991). Composition and mechanics of routine swimming of rainbow trout, *Oncorhynchus mykiss*. *Can. J. Fish. Aquat. Sci.* **48**, 583–590.

Webb, P. W. (1994). Exercise performance of fish. In *Advances in Veterinary Science and Comparative Medicine*, vol. 38B, *Comparative Vertebrate Exercise Physiology: Phyletic Adaptations* (ed. J. H. Jones), pp. 1–49. San Diego: Academic Press.

Webb, P. W. and Blake, R. W. (1985). Swimming. In *Functional Vertebrate Morphology* (ed. M. Hildebrand, D. M. Bramble, K. F. Liem and D. B. Wake), pp. 110–128. Cambridge: Harvard University Press.

Webb, P. W., LaLiberte, G. D. and Schrank, A. J. (1996). Does body and fin form affect the maneuverability of fish traversing vertical and horizontal slits? *Env. Biol. Fish.* **46**, 7–14.

Webb, P. W. and Weihs, D. (1994). Hydrostatic stability of fish with swim bladders: not all fish are unstable. *Can. J. Zool.* **72**, 1149–1154.

Weihs, D. (1972). A hydrodynamic analysis of fish turning manoeuvres. *Proc. R. Soc. Lond. B* **182**, 59–72.

Westneat, M. W. (1996). Functional morphology of aquatic flight in fishes: kinematics, electromyography, and mechanical modeling of labriform locomotion. *Am. Zool.* **36**, 582–598.

Wilga, C. D. and Lauder, G. V. (1999). Locomotion in sturgeon: function of the pectoral fins. *J. Exp. Biol.* **202**, 2413–2432.

Wilga, C. D. and Lauder, G. V. (2000). Three-dimensional kinematics and wake structure of the pectoral fins during locomotion in leopard sharks, *Triakis semifasciata*. *J. Exp. Biol.* **203**, 2261–2278.

Willert, C. E. and Gharib, M. (1991). Digital particle image velocimetry. *Exp. Fluids* **10**, 181–193.

Wolfgang, M. J., Anderson, J. M., Grosenbaugh, M., Yue, D. and Triantafyllou, M. (1999). Near-body flow dynamics in swimming fish. *J. Exp. Biol.* **202**, 2303–2327.